SESSION 6b.

NONLINEAR ANALYSIS

Session Chairman

R. W. Leonard

NASA Langley Research Center
Hampton, Virginia

AFFDL-TR-68-150

AN APPROXIMATE NONLINEAR ANALYSIS OF THIN PLATES

D. W. Murray*
University of Alberta, Edmonton, Canada

E. L. Wilson*
University of California, Berkeley, California

An approximate finite element formulation for solution of thin plate problems including geometric and material nonlinearities is presented. Material properties are assumed to be represented by an effective stress-effective strain generalization of a uniaxial tension test. The method approximates the stiffness of the element by assuming material response throughout the element is governed by the variation of effective strains through the thickness at the centroid. Tangent and secant stiffness may then be determined from the linear elastic membrane and bending stiffness by simple one-dimensional numerical integration. Illustrative results are given for cylindrical bending of simply supported plate strips.

*Associate Professor of Civil Engineering

SECTION I

INTRODUCTION

Many recent developments have taken place in the field of finite element analysis of nonlinear problems. Reference to much of this work is contained in a paper by Mallett and Marcal (Reference 1). The present paper extends an approach used by the authors, in solving large deflection plate problems (Reference 2) and investigating post-buckling behavior of plates (Reference 3), to include an approximate technique for incorporating nonlinear material response.

The general solution technique and derivation of linear elastic element stiffnesses has been described in detail in Reference 2. It includes the effect of changes in geometry on the equilibrium equations and the effect of nonlinear strain-displacement terms arising from element rotations. The approach is incremental and iterative and is based on achieving an equilibrium balance between element resisting forces and applied loads. Since the procedure is iterative the stiffness matrix need not be exact.

The effect of initial stress on the incremental structure stiffness has been discussed in detail in Reference 3. This gives rise to the so-called "geometric stiffness" matrix which results in a better approximation of the incremental stiffness and therefore reduces the number of iterations required to achieve an equilibrium balance.

SECTION II

PRELIMINARY DEVELOPMENT

The analysis is formulated for a triangular element utilizing the shape functions associated with the constant strain triangle (Reference 4) for membrane displacements and those associated with the Hsieh-Clough-Tocher triangle (Reference 5) for bending displacements.

The global coordinate system, global displacements and global displacement increments are designated by the upper case letters X_i, $\bar{U}_i$ and U_i (or X, Y, Z; $\bar{U}$, $\bar{V}$, $\bar{W}$; and, U, V, W), respectively. Local coordinate systems, local displacements, and increments in local displacements are designated by the lower case letters x_i, $\bar{u}_i$ and u_i (or x, y, z; $\bar{u}$, $\bar{v}$, $\bar{w}$; and, u, v, w), respectively. This nomenclature is illustrated in Figure 1. Rectangular cartesian coordinates are used throughout.

The incremental equilibrium equation, expressing the equilibrium requirement for the structure in the "incremented" configuration $\Gamma + \Delta\Gamma$, may be derived by taking the difference between the virtual displacement equations, for configuration $\Gamma + \Delta\Gamma$ and for the 'initial' equilibrium configuration Γ (Figure 1). The resulting equation, derived in Reference 3, is

$$\sum \frac{1}{2} \int_{V_o} S_{ij} \; \delta (u_{k,i} \;\; u_{k,j}) \, dV_o + \sum \int_{V_o} \Delta S_{ij} \, \delta (\Delta E_{ij}) \, dV_o = \sum \int_{S_o} \Delta T_i \; \delta U_i \;\; dS_o \qquad (1)$$

where, S_{ij} and ΔS_{ij} are the Kirchhoff stress tensor in position Γ and the increments in the Kirchhoff stress tensor due to $\Delta\Gamma$, respectively; ΔE_{ij} is the increment in Green's strain tensor due to $\Delta\Gamma$ and may be expressed by

$$2\Delta E_{ij} = u_{i,j} + u_{j,i} + u_{k,i} \;\; u_{k,j} + \bar{u}_{k,i} \;\; u_{k,j} + u_{k,i} \;\; \bar{u}_{k,j} \qquad (2)$$

δ indicates a virtual variation of the displacement increments; ΔT_i are increments in the surface tractions corresponding to $\Delta\Gamma$; and, dV_o and dS_o are elements of volume and area in the 'original' configuration. The summation indicates the integrals are evaluated over separate subregions of the structure and then combined for the entire structure.

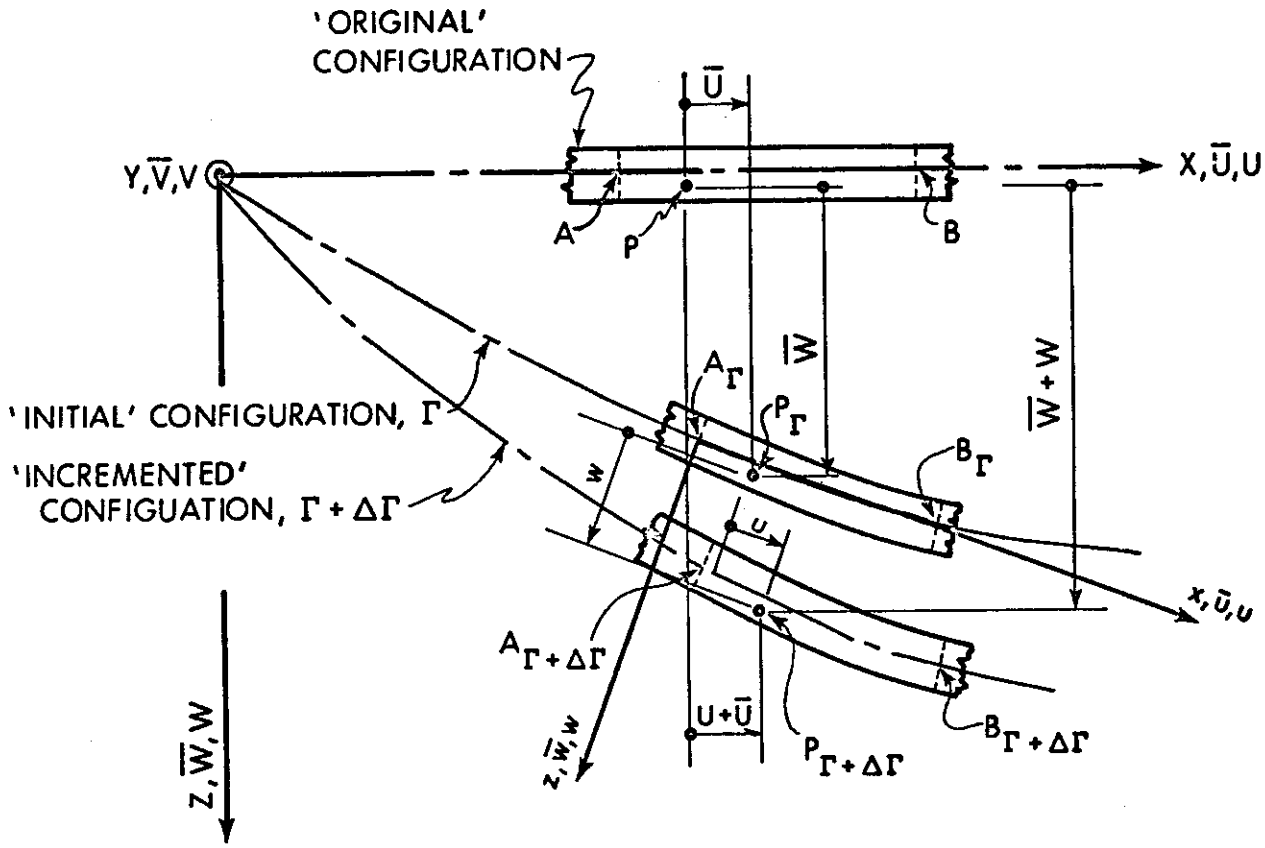

GLOBAL COORDINATES	X_i	$\rightarrow \{X,Y,Z\}$
'INITIAL' GLOBAL DISPLACEMENTS	$\bar{U}_i$	$\rightarrow \{\bar{U},\bar{V},\bar{W}\}$
GLOBAL DISPLACEMENT INCREMENTS	U_i	$\rightarrow \{U,V,W\}$
LOCAL COORDINATES	x_i	$\rightarrow \{x,y,z\}$
'INITIAL' LOCAL DISPLACEMENTS	$\bar{u}_i$	$\rightarrow \{\bar{u},\bar{v},\bar{w}\}$
LOCAL DISPLACEMENT INCREMENTS	u_i	$\rightarrow \{u,v,w\}$

Figure 1. Coordinate and Displacement Nomenclature

In utilizing equation 1 to arrive at a stiffness formulation, the integrals are evaluated over each subregion (element). Displacements* are referred to the local coordinate system, which is established by the element position in configuration Γ. Using the Kirchhoff assumptions, element displacements may be expressed in terms of nodal displacements by the relationship**.

$$\begin{Bmatrix} \tilde{u} \\ \tilde{v} \\ \tilde{w} \end{Bmatrix} = \begin{bmatrix} \{\phi_u\}^T & \cdot & -z\{\phi_w\}^T_{,x} \\ \cdot & \{\phi_v\}^T & -z\{\phi_w\}^T_{,y} \\ \cdot & \cdot & \{\phi_w\}^T \end{bmatrix} \begin{Bmatrix} \{u\} \\ \{v\} \\ \{w\} \end{Bmatrix} \tag{3}$$

where, $\tilde{u}$, $\tilde{v}$ and $\tilde{w}$ are displacements in the coordinate directions; $\{u\}$, $\{v\}$ and $\{w\}$ are the nodal displacement vectors associated with the middle surface of the plate, illustrated in Figure 2; and $\{\phi_u\}$, $\{\phi_v\}$ and $\{\phi_w\}$ are the vectors of interpolating functions associated with the respective nodal displacement vectors $\{u\}$, $\{v\}$ and $\{w\}$.

Substitution of Equation 3 into Equation 1 allows Equation 1 to be expressed in matrix form, in terms of a finite number of nodal displacements, when the element nodal displacements are transformed to the global system and identified with the 'structure' nodal displacements. This yields an equation of the form

$$\{\delta \Delta r\}^T \left[[K_G] + [K_T] \right] \{\Delta r\} = \{\delta \Delta r\}^T \{\Delta R\} \tag{4}$$

In Equation 4, $[K_G]$ is the geometric stiffness matrix. It has been evaluated in Reference 3. For linear elastic material response, $[K_T]$, is the normal assembled structural stiffness matrix. The subscript, T, is used here to indicate it is a tangent stiffness when nonlinear material response is considered. The vectors $\{\Delta r\}$ and $\{\Delta R\}$ represent the increments in global nodal displacement and loading vectors associated with the assembled structure. Recognizing that the virtual displacements are arbitrary, the incremental equilibrium Equation 4 may be written as

$$[K_I] \{\Delta r\} = \{\Delta r\} \tag{5}$$

where $[K_I]$ will be referred to as the incremental stiffness matrix and results after combining $[K_G]$ and $[K_T]$.

*The term 'displacements' should be interpreted as 'displacement increments' in the following discussion. The word 'increment' is omitted for the sake of brevity.

**A tilde (~) is used hereafter to differentiate field variables from nodal values, except for the case of interpolation functions.

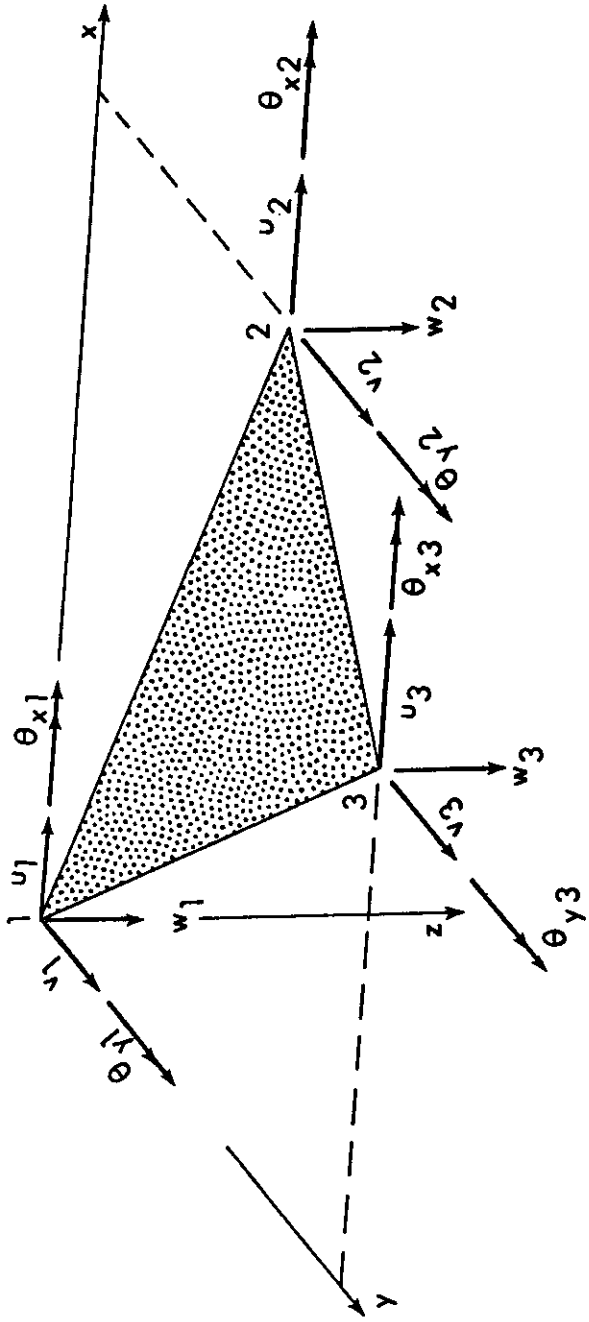

$$\{u\}^T \equiv \langle u_1 \; u_2 \; u_3 \rangle \quad ; \quad \{v\}^T \equiv \langle v_1 \; v_2 \; v_3 \rangle \; ; \; \{r_p\}^T \equiv \langle \{u\}^T \; \{v\}^T \rangle$$

$$\{r_B\}^T \equiv \{w\}^T = \langle w_1 \; \theta_{x1} \; \theta_{y1} \; w_2 \; \theta_{x2} \; \theta_{y2} \; w_3 \; \theta_{x3} \; \theta_{y3} \rangle$$

Figure 2. Nodal Displacements and Nodal Vectors

SECTION III

THE ELEMENT TANGENT STIFFNESS

The principal purpose of this paper is to develop an approximate method of evaluating the element stiffnesses contributing to $[K_T]$ of Equation 4. This requires the evaluation of the second term of Equation 1 for each element. For a plate element subject to Kirchhoff's assumptions, the variables in this term may be specialized and only the nonzero strain components need be retained. Since it is assumed that for any element the engineering strains, and displacement gradients with respect to the element coordinates, remain 'small', the product terms in Equation 2 may be discarded and the second term of Equation 1 may be written in terms of increments of engineering strains and stresses,* as

$$\int_{V_0} \{\tilde{\epsilon}^*\}^T \{\tilde{\sigma}\}\, dV_0 \tag{6}$$

where

$$\{\tilde{\epsilon}\} \equiv \begin{Bmatrix} \tilde{\epsilon}_x \\ \tilde{\epsilon}_y \\ \tilde{\gamma}_{xy} \end{Bmatrix} = \begin{Bmatrix} \dfrac{\partial \tilde{u}}{\partial x} \\ \dfrac{\partial \tilde{v}}{\partial y} \\ \dfrac{\partial \tilde{u}}{\partial y} + \dfrac{\partial \tilde{v}}{\partial x} \end{Bmatrix} \tag{7}$$

and

$$\{\tilde{\sigma}\} \equiv \begin{Bmatrix} \tilde{\sigma}_x \\ \tilde{\sigma}_y \\ \tilde{\tau}_{xy} \end{Bmatrix} = [\tilde{C}]\,\{\tilde{\epsilon}\} \tag{8}$$

In Equation 8, the matrix $[\tilde{C}]$ represents a two dimensional constitutive relationship which specifies increments in stress in terms of increments in strain. In general this matrix will vary throughout the volume of the element.

*An asterisk (*) will hereafter be used to designate a virtual variation of a displacement quantity.

Substitution of the displacement expression (Equation 3) into Equation 7 yields

$$\{\tilde{\epsilon}\} = \left[\begin{array}{cc|c} \{\phi_u\}^T_{,x} & \cdot & -z\{\phi_w\}^T_{,xx} \\ \cdot & \{\phi_v\}^T_{,y} & -z\{\phi_w\}^T_{,yy} \\ \{\phi_u\}^T_{,y} & \{\phi_v\}^T_{,x} & -2z\{\phi_w\}^T_{,xy} \end{array}\right] \left\{\begin{array}{c} \{u\} \\ \{v\} \\ \{w\} \end{array}\right\} \tag{9}$$

It is convenient to write Equation 9 in terms of increments in middle surface strains and curvatures, $\{\tilde{\epsilon}_o\}$ and $\{\tilde{\mathcal{K}}\}$, respectively, which can be done by the indicated partitioning of the equation. This yields*

$$\{\tilde{\epsilon}\} = \left[\tilde{B}_P \mid -z\tilde{B}_B\right] \left\{\begin{array}{c} r_P \\ \hline r_B \end{array}\right\} \tag{10}$$

or

$$\{\tilde{\epsilon}\} = \{\tilde{\epsilon}_o\} - z\{\mathcal{K}\} \tag{11}$$

where terms in Equations 10 and 11 are defined by identification with corresponding terms in the preceding equations. The subscripts P and B in Equation 10 indicate quantities associated with in-plane behavior and bending behavior respectively.

Upon utilizing Equations 11 and 8, Expression 6 becomes

$$\int_{V_o} \left\{\{\tilde{\epsilon}_o^*\} - z\{\tilde{\mathcal{K}}^*\}\right\}^T [\tilde{C}] \left\{\{\tilde{\epsilon}_o\} - z\{\mathcal{K}\}\right\} dV_o \tag{12}$$

and evaluating $\{\tilde{\epsilon}_o\}$ and $\{\mathcal{K}\}$ in terms of nodal displacement increments, (Equation 10), yields

$$\left\{\begin{array}{c} r_P^* \\ \hline r_B^* \end{array}\right\}^T \int_{V_o} \left[\begin{array}{c|c} \tilde{B}_P^T \tilde{C} \tilde{B}_P & -z\tilde{B}_P^T \tilde{C} \tilde{B}_B \\ \hline -z\tilde{B}_B^T \tilde{C} \tilde{B}_P & z^2 \tilde{B}_B^T \tilde{C} \tilde{B}_B \end{array}\right] dV_o \left\{\begin{array}{c} r_P \\ \hline r_B \end{array}\right\} \tag{13}$$

*Where submatrices or subvectors are obviously matrices or vectors, the brackets or braces have been omitted in the following.

The quantity within the integral represents the element tangent stiffness, designated by $[K_{ET}]$, and can be written symbolically as

$$[K_{ET}] = \left[\begin{array}{c|c} K_{PP} & K_{PB} \\ \hline K_{BP} & K_{BB} \end{array}\right] \tag{14}$$

where submatrices are defined by identification with the corresponding terms in Expression 13.

For linear elastic material response the in-plane and bending effects uncouple, since the coupling terms are linearly dependent on z, and yield the stiffness matrices associated with linear elastic in-plane and bending behavior. These matrices are designated as $[K_E]$, $[K_p]$ and $[K_B]$ and are related by the equation

$$[K_E] = \left[\begin{array}{c|c} K_P & \cdot \\ \hline \cdot & K_B \end{array}\right] \tag{15}$$

The matrices $[K_p]$ and $[K_B]$ have been evaluated many times (e.g. References 4 and 5).

In general, the evaluation of the element tangent stiffness requires a volume integration as indicated in Expression 13. If the incremental constitutive relationship is a function of the strain history, as is the case in elastic-plastic analysis, the numerical computations involved are prohibitive for any extensive analysis. In addition, many displacement models (including the model for this analysis) have strain discontinuities. It is therefore questionable whether the effort involved in maintaining complete consistency between element strains and the constitutive relationship is justified unless applied to a higher order element. The tangent stiffness has therefore been approximated in this analysis by relating material properties to strains at the centroid of the element. This results in considerable simplication but indicates a fine subdivision of the structure is required to adequately simulate behavior.

SECTION IV

A NONLINEAR CONSTITUTIVE HYPOTHESIS

There are a large number of constitutive relationships which may be utilized in evaluating the tangent stiffness matrix of Equations 13 and 14. Khojasteh-Bakht (Reference 6) and Marcal and Pilgrim (Reference 7) have derived constitutive equations for elastic-plastic response in a form which may be conveniently used in evaluation of tangent stiffnesses.

In view of the approximations involved, however, it was considered reasonable to adopt a simpler set of nonlinear elastic relationships which can be assumed to approximately simulate elastic-plastic behavior. This in no way restricts the general approach to the problem.

Since initiation of yielding of metals has been shown to be essentially independent of dilatation, the yield surface at which plastic response is initiated is generally related to the strain invariant,

$$\pi_\epsilon = (\epsilon_1 - \epsilon_2)^2 + (\epsilon_2 - \epsilon_3)^2 + (\epsilon_3 - \epsilon_1)^2$$
$$= (\epsilon_x - \epsilon_y)^2 + (\epsilon_y - \epsilon_z)^2 + (\epsilon_z - \epsilon_x)^2 + \frac{3}{2}(\gamma_{xy}^2 + \gamma_{yz}^2 + \gamma_{zx}^2) \qquad (15a)$$

For an elastic-plastic hardening material it may be hypothesized, in a 'deformation theory', that an effective stress, defined as

$$\bar{\sigma} = \frac{1}{\sqrt{2}}\left[(\sigma_x - \sigma_y)^2 + (\sigma_y - \sigma_z)^2 + (\sigma_z - \sigma_x)^2 + 6(\tau_{xy}^2 + \tau_{yz}^2 + \tau_{zx}^2)\right]^{1/2} \qquad (16)$$

is related to an effective plastic strain, defined as

$$\bar{\epsilon}^P = \frac{\sqrt{2}}{3}\sqrt{\pi_\epsilon^P} \qquad (17)$$

The definitions of the effective quantities are obtained by equating the second stress and plastic strain invariants to the values of these quantities in a simple tension test. The relationship between the generalized expressions for $\bar{\sigma}$ and $\bar{\epsilon}$ is then assumed to be that observed in a simple tension test.

For this analysis it was hypothesized that a nonlinear elastic relationship existed such that the elastic modulus could be obtained from a uniaxial tension test which relates effective

stress to effective total strain. Proceeding in a manner identical to that used above we derive an expression for effective stress which is identical to Equation 16 while the effective strain becomes

$$\bar{\epsilon} = \frac{1}{\sqrt{2}\,(1+\nu)} \sqrt{\pi_\epsilon} \tag{18}$$

Assuming uniaxial tension test results as illustrated in Figure 3, the general two dimensional constitutive relationship may then be considered to be

$$\left\{\tilde{\sigma}\right\} = \frac{E_T}{E} \left[C\right] \left\{\tilde{\epsilon}\right\} \tag{19}$$

where $\left\{\tilde{\sigma}\right\}$ and $\left\{\tilde{\epsilon}\right\}$ are the vectors of stress and strain increments defined in Equations 7 and 8, E is the elastic modulus, E_T is the tangent modulus from the uniaxial tension test, and $\left[C\right]$ is the linear elastic two dimensional plane stress constitutive relationship, which is

$$\left[C\right] = \frac{E}{1-\nu^2} \begin{bmatrix} 1 & \nu & \cdot \\ \nu & 1 & \cdot \\ \cdot & \cdot & \frac{1-\nu}{2} \end{bmatrix} \tag{20}$$

Equation 19 defines the matrix $\left[\tilde{C}\right]$ of Equation 8 for the present hypothesis. Specializing Equations 16 and 17 for a plane stress condition yields the specific forms of $\bar{\sigma}$ and $\bar{\epsilon}$ which apply to this problem.

In addition to the tangent stiffness constitutive relationship, it is also possible to define a secant stiffness matrix, which relates final stresses to total strains, as

$$\left[\tilde{C}_s\right] = \frac{E_s}{E} \left[C\right] \tag{21}$$

where E_s is the secant modulus (Figure 3). This constitutive matrix was utilized in evaluating the element equilibrating forces which are necessary in performing the equilibrium check as discussed in Reference 2.

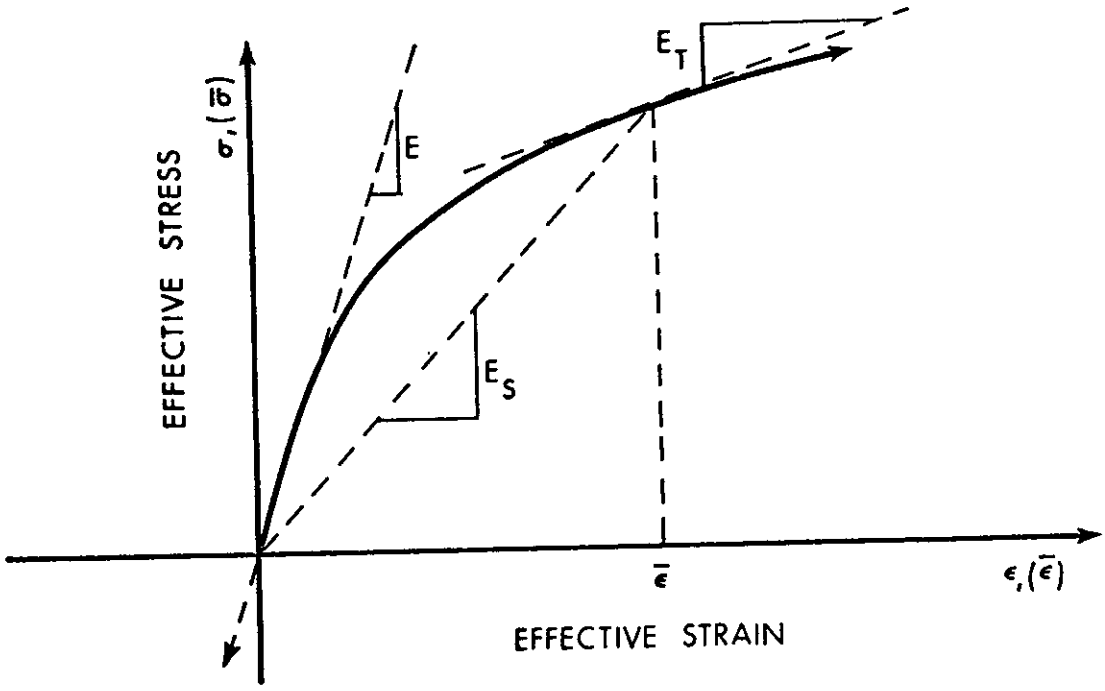

Figure 3. Generalized Stress-Strain Curve

SECTION V

EVALUATION OF TANGENT AND SECANT STIFFNESSES

By virtue of the assumption that the constitutive matrix for the entire element is related to strains at the centroid of the element, the matrix $[\tilde{C}]$ is a function of the z spatial coordinate only. This permits a simple evaluation of the element tangent and secant stiffnesses. Defining a new coordinate η in the z direction by the relationship

$$\eta = z - b \tag{22}$$

where b is a constant, Expression 12 becomes

$$\begin{aligned}&\int_{V_0} \left\{\{\tilde{\epsilon}_0^*\} - b\{\tilde{\mathcal{H}}^*\}\right\}^T [\tilde{C}] \left\{\{\tilde{\epsilon}_0\} - b\{\tilde{\mathcal{H}}\}\right\} dV_0 \\ &+ \int_{V_0} \eta^2 \{\tilde{\mathcal{H}}^*\}^T [\tilde{C}] \{\mathcal{H}\} dV_0 - \int_{V_0} \eta \{\tilde{\mathcal{H}}^*\}^T [\tilde{C}] \left\{\{\epsilon_0\} - b\{\mathcal{H}\}\right\} dV_0 \\ &- \int_{V_0} \eta \left\{\{\tilde{\epsilon}_0^*\} - b\{\tilde{\mathcal{H}}^*\}\right\}^T [\tilde{C}] \{\tilde{\mathcal{H}}\} dV_0\end{aligned} \tag{23}$$

Since $[\tilde{C}]$ is a function of z or η only, and may be expressed in the form of Equation 19, where E_T is the variable, the constant b may be selected as

$$b = \frac{\int_h z E_T(z) dz}{\int_h E_T(z) dz} \tag{24}$$

where h is the thickness of the plate. Cross multiplying Equation 24 and grouping the two terms indicates that this definition of b produces the result

$$\int_h \eta E_T(z) dz = 0 \tag{25}$$

In addition, the vector $\{\tilde{\epsilon}_0\} - b\{\tilde{\mathcal{H}}\}$ represents the strains on the surface z = b and can therefore be represented as $\{\tilde{\epsilon}_b\}$. By virtue of Equation 25 the last two terms in Expression 23 drop out and Expression 23 reduces to

$$\int_{V_0} \{\tilde{\epsilon}_b^*\}^T [\tilde{C}] \{\tilde{\epsilon}_b\} dV_0 + \int_{V_0} \eta^2 \{\tilde{\mathcal{H}}^*\}^T [\tilde{C}] \{\tilde{\mathcal{H}}\} dV_0 \tag{26}$$

Using Equations 10 and 11 to express $\{\tilde{\epsilon}_b\}$ and $\{\tilde{\chi}\}$ in terms of nodal displacements,* Expression 26 becomes

$$\begin{Bmatrix} r^*_{Pb} \\ r^*_B \end{Bmatrix}^T \int_{V_o} \left[\begin{array}{c|c} \tilde{B}_P^T \tilde{C} \tilde{B}_P & \cdot \\ \hline & \eta^2 \tilde{B}_B^T \tilde{C} \tilde{B}_B \end{array}\right] dV_o \begin{Bmatrix} r_{Pb} \\ r_B \end{Bmatrix} \tag{27}$$

where $\{r_{Pb}\}$ is the vector of in-plane nodal displacements on the plane z = b. The in-plane and bending stiffnesses uncouple at the reference plane z = b by virtue of the definition of b and such a plane may be referred to as the "plane of stiffness". On this surface, increments of in-plane displacements produce no stress couples and increments of bending displacements produce no stress resultants for the particular variation of the constitutive modulus.

The stiffness submatrices appearing in Expression 27 may be evaluated by integrating through the thickness of the plate and are directly related to the linear elastic matrices of Equation 15 by the equations

$$[K_{Pb}] \equiv \int_{V_o} \tilde{B}_P^T \tilde{C} \tilde{B}_P \, dV_o = \frac{\int_h E_T(\eta)\, d\eta}{Eh} [K_P] \tag{28}$$

and

$$[K_{Bb}] \equiv \int_{V_o} \eta^2 \tilde{B}_B^T \tilde{C} \tilde{B}_B \, dV_o = \frac{12 \int_h \eta^2 E_T(\eta) d\eta}{Eh^3} [K_B] \tag{29}$$

In order to assemble these stiffness matrices it is now necessary to relate the nodal vectors of Expression 27 to the nodal vectors on the middle surface as they appear in Expression 13. This can be accomplished by expressing the vector $\{r_{Pb}\}$ as

$$\{r_{Pb}\} = \{r_P\} - b \begin{Bmatrix} \{\theta_y\} \\ -\{\theta_x\} \end{Bmatrix} = \{r_P\} - b\{\theta\} \tag{30}$$

where $\{\theta_y\}$ and $\{\theta_x\}$ are the vectors of corresponding nodal rotations appearing in $\{r_B\} = \{w\}$ defined in Figure 2.

*It is assumed here that interpolation functions apply on the plane z = b and not on the plane z = o.

Substitution of Equation 30 into Expression 27 yields

$$\left\{\begin{array}{c} r_P^* \\ \hline r_B^* \end{array}\right\} = \left[\begin{array}{c|c} \alpha K_P & -b\,K_{P\theta} \\ \hline -b\,K_{\theta P} & \beta\,K_B + b^2\,K_{\theta\theta} \end{array}\right] \left\{\begin{array}{c} r_P \\ \hline r_B \end{array}\right\} \tag{31}$$

where α is the coefficient of K_p in Equation 28, β is the coefficient of K_B in Equation 29, b is defined by Equation 24 and $K_{P\theta}$, $K_{\theta p}$ and $K_{\theta\theta}$ have elements identical to those of αK_p but with rows and columns of zeros inserted, and the appropriate sign changes from Equation 30, so that elements of the vector $\{\theta\}$ are identified with the corresponding elements of $\{r_B\}$.

The submatrices of Expression 31 may now be identified with the submatrices of Equation 14. The element tangent matrix has now been completely determined. It can be evaluated in terms of the linear elastic stiffness matrices of Equation 15 once α, β and b have been determined. These can be evaluated by simple numerical integration through the thickness of the plate.

The element secant stiffness may be evaluated in the same way when $E_T(\eta)$ is replaced by $E_S(\eta)$.

SECTION VI

SOLUTION PROCEDURE AND EXAMPLES

The approximate formulation developed above was applied to determine the interaction of membrane and bending resistance of some simply supported plate strips. The assumed material properties, which exhibit a "softening" at an effective strain of 0.00135, are shown in the effective stress-effective strain curve of Figure 4.

A schematic illustration of the solution procedure is shown in Figure 5. To a given configuration Γ, described by global nodal displacements r_Γ and maintaining equilibrium with the loads R_Γ, a load increment $\Delta R = R_{\Gamma+\Delta\Gamma} - R_\Gamma$ is applied. Geometric and tangent element stiffnesses are evaluated, transformed to global orientation and assembled to form the incremental stiffness of the structure. The increments in nodal displacements are approximated by solving Equation 5, which has the form

$$\left[K_I^\Gamma \right] \left\{ \Delta r' \right\} = \left\{ \Delta R \right\} \tag{32}$$

for $\left\{ \Delta r' \right\}$

Incrementing the nodal displacements produces the configuration r^2. For this configuration, element deformations, and from these, element secant stiffnesses are evaluated to determine the element equilibrating forces. Transforming to global orientation, assembling and subtracting the structure equilibrating forces from the applied forces, determines the unbalanced forces R_u^2 acting on the current configuration. A new set of displacement increments is now determined by solving for $\left\{ \Delta r^2 \right\}$ in the equation

$$\left[K_I^\Gamma \right] \left\{ \Delta r^2 \right\} = \left\{ R_u^2 \right\} \tag{33}$$

The process is repeated until the equilibrium configuration $\Gamma + \Delta\Gamma$ is established. The next load increment is then applied and the solution progresses in the same way.

Figure 6 compares a moment-curvature curve computed in this way with a closed form evaluation.

Figures 7 and 8 give results for an infinite strip of simply supported plate, deformed into a cylindrical configuration by applying a line load along the center line. The plate has a

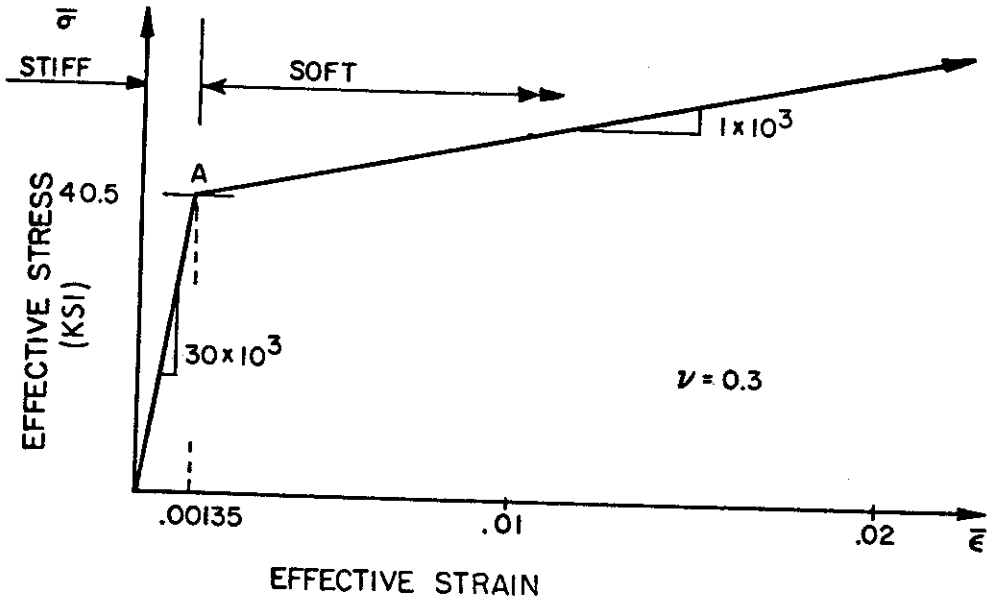

Figure 4. Assumed Material Properties

span to thickness ratio of 28 and the largest center deflection is equal to the plate thickness. Figure 7 indicates the rapid dominance of membrane behavior. Figure 8 indicates the progress of the 'softened' zones, the stress distribution and the plate profiles.

Figures 9 and 10 give similar results for a plate, with a span to thickness ratio of 140, up to a center deflection of five times the plate thickness. At load increment five, softening had progressed into the bottom of the plate along the line of maximum moment (Figure 10). At load increment seven the entire plate had softened except for a small region in the neighborhood of the applied load. At this point the plate was stretching "like a rubber band". Some difficulty was encountered with convergence in this region as indicated on Figure 9.

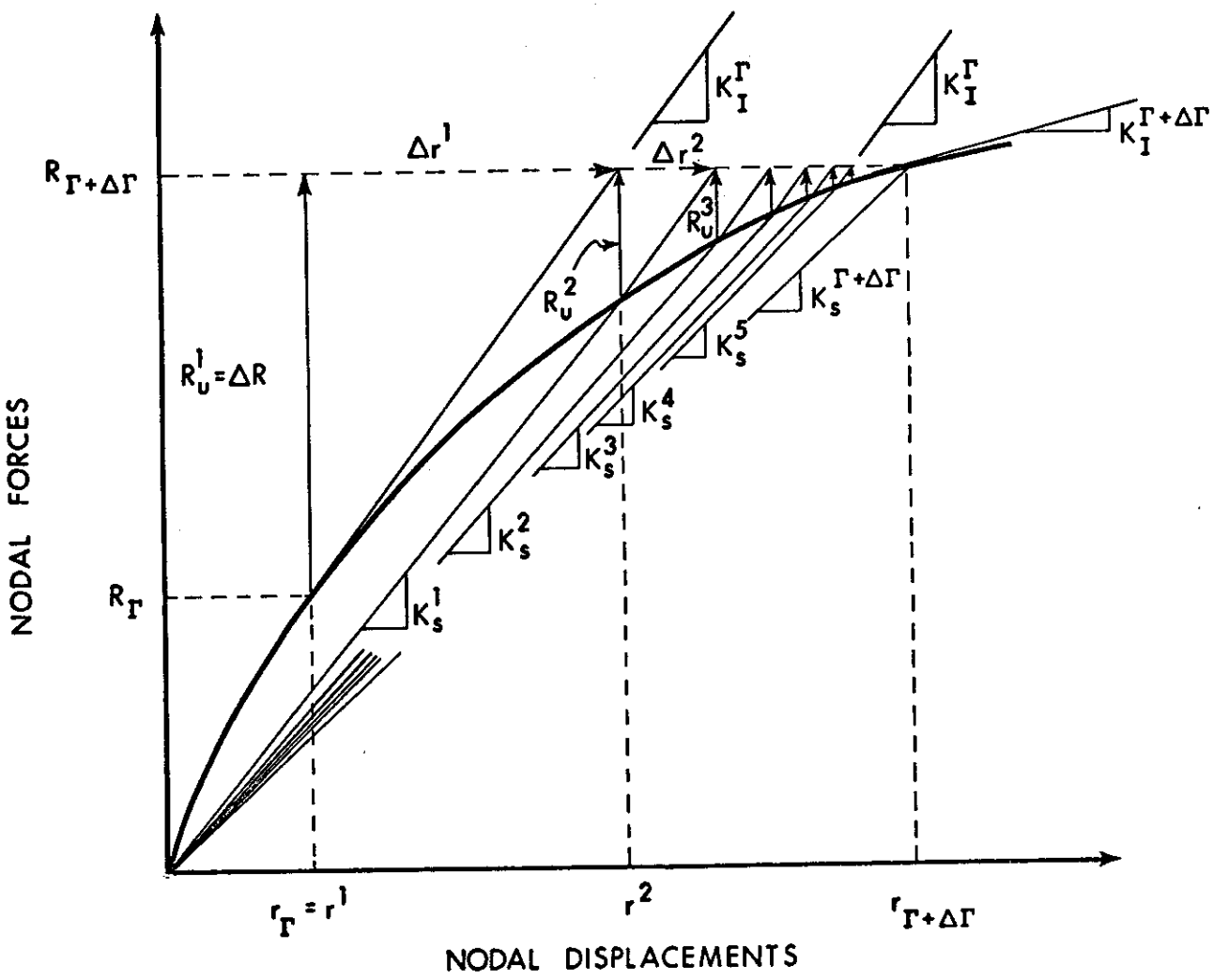

Figure 5. Solution Procedure

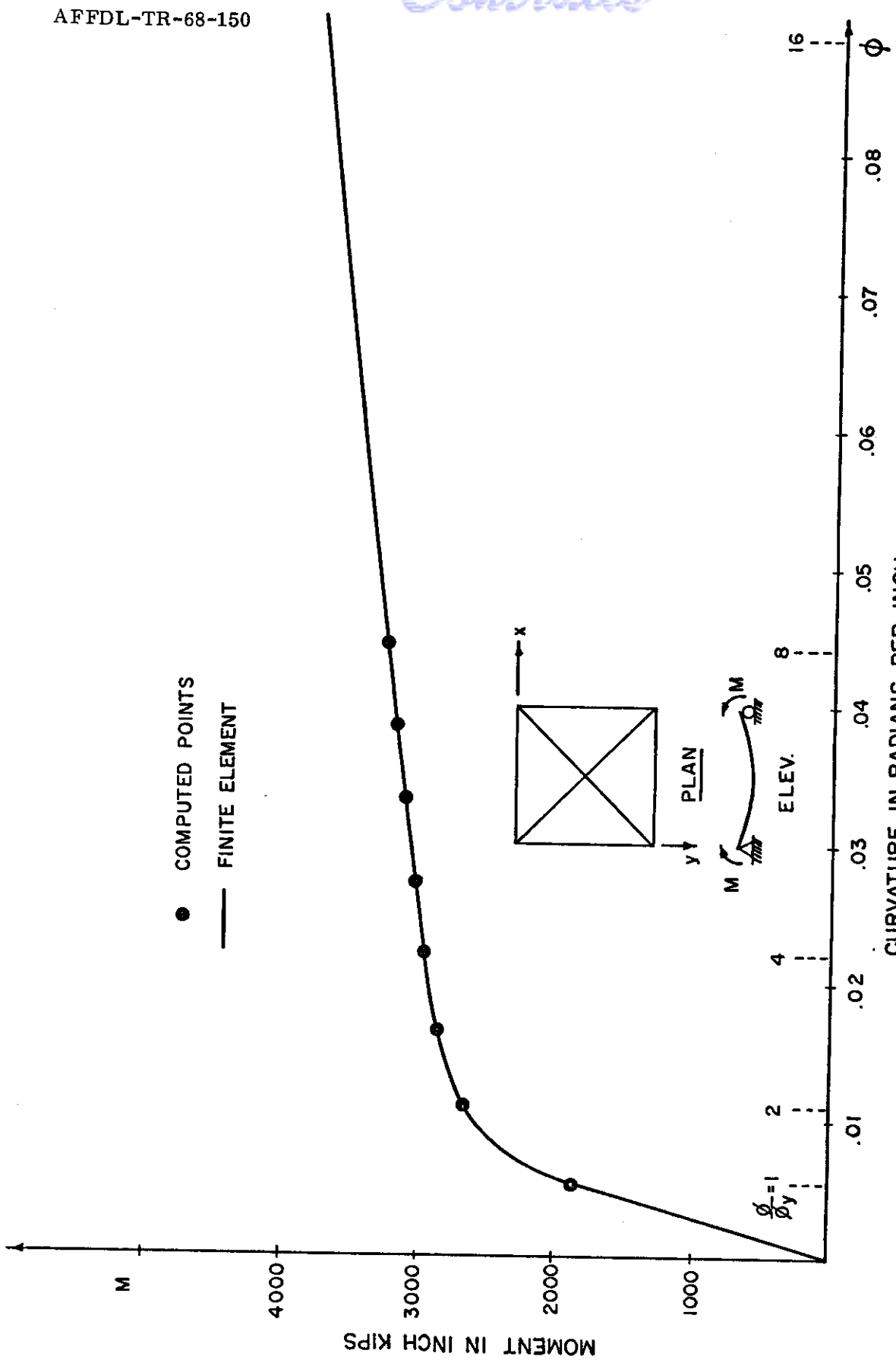

Figure 6. Moment Curvature for 1/2 Plate

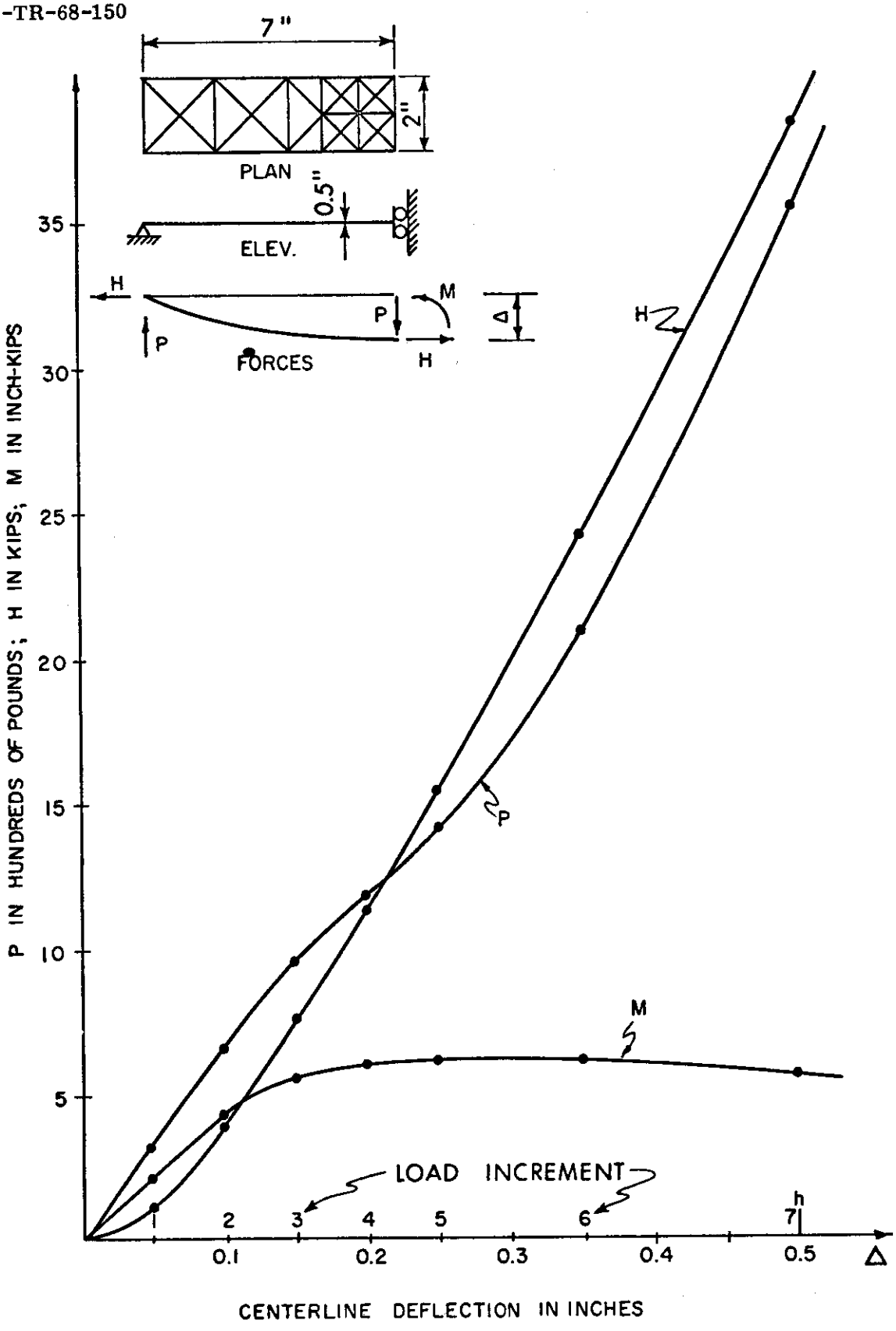

Figure 7. Force Deflection for Cylindrical Bending of 2"x14"x0.5" Plate

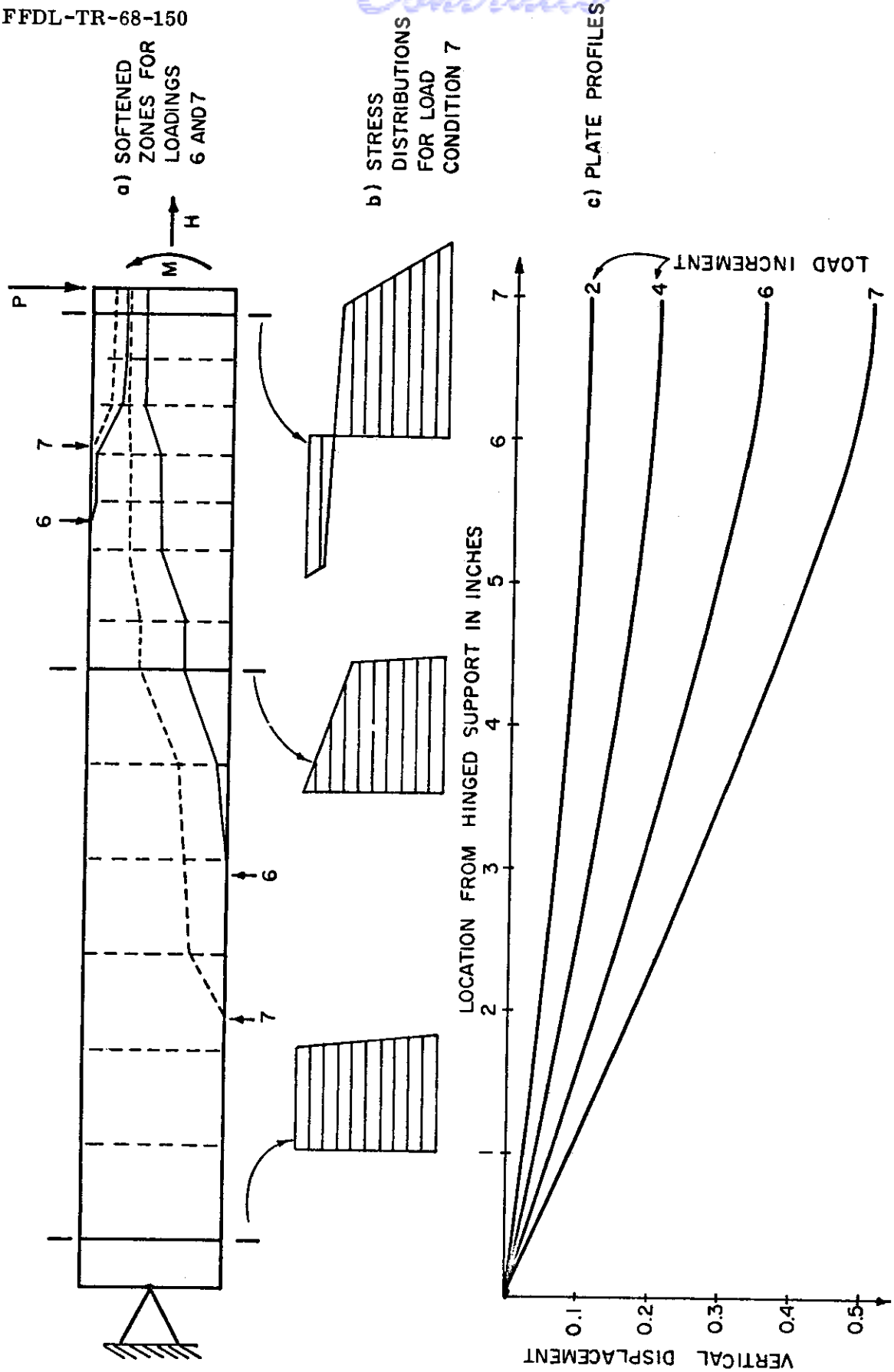

Figure 8. Stresses and Profiles for Cylindrical Bending of 2" x14" x0.5" Plate

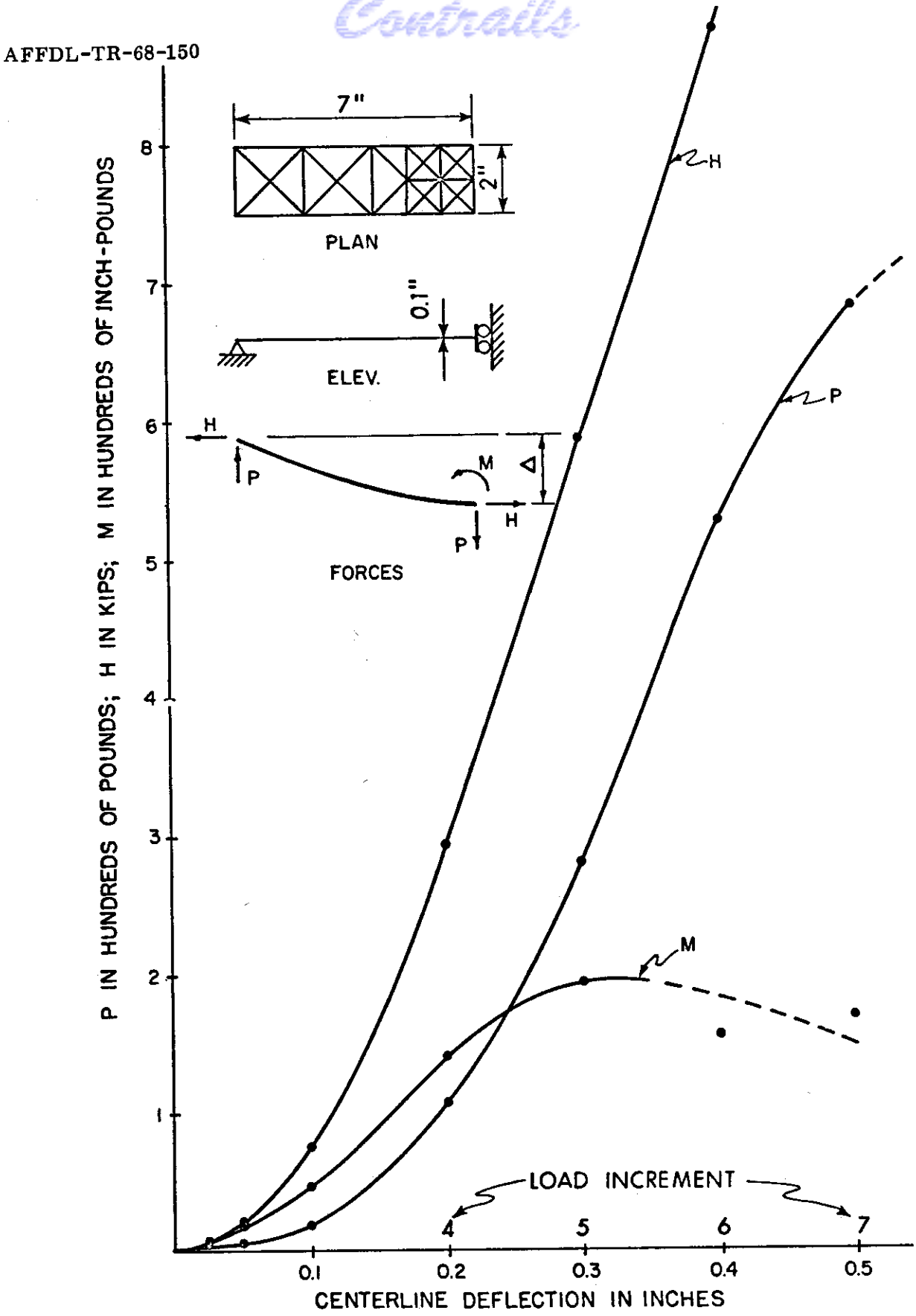

Figure 9. Force Deflection for Cylindrical Bending of 2 x 14 x 0.1 Inch Plate

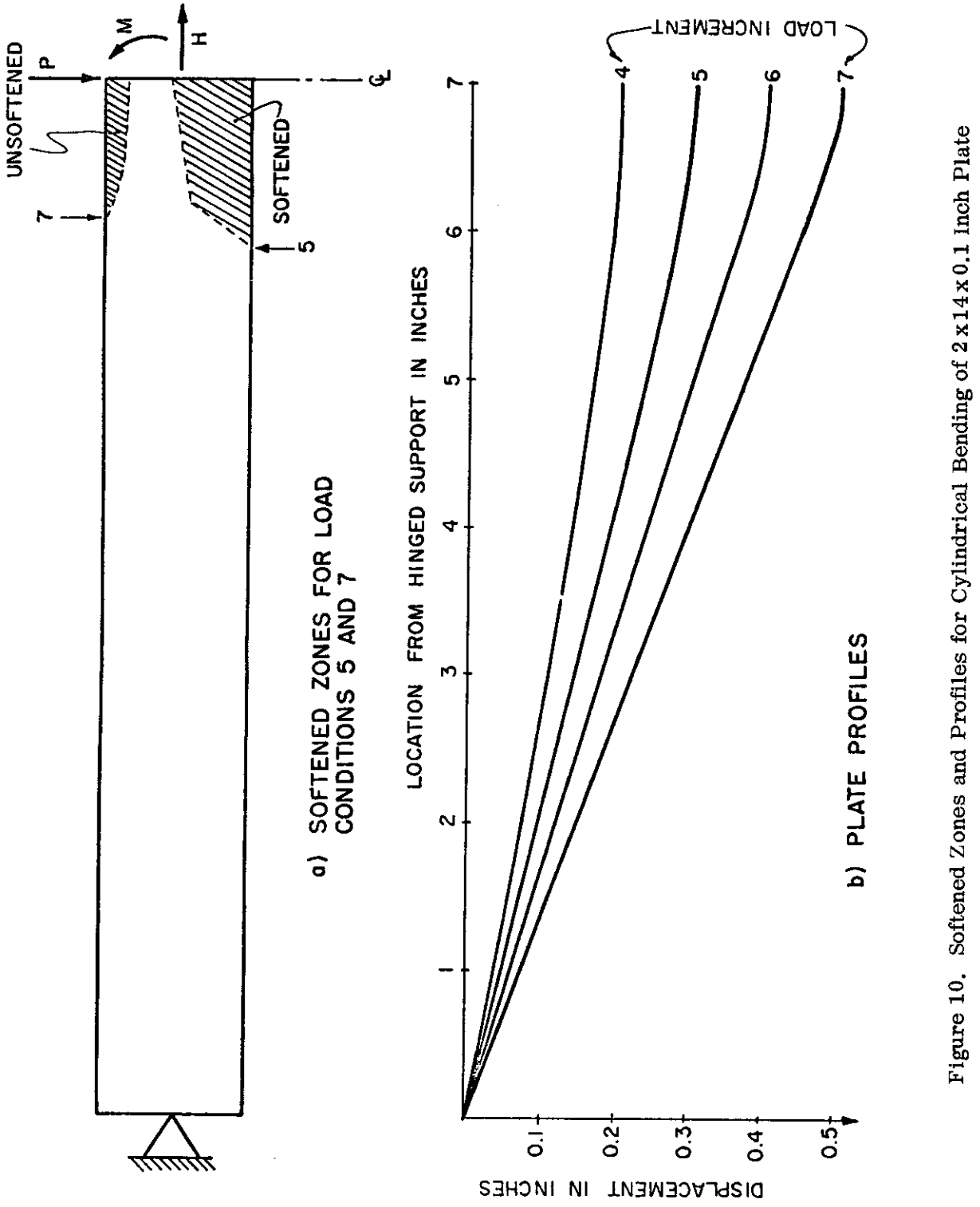

Figure 10. Softened Zones and Profiles for Cylindrical Bending of 2 x 14 x 0.1 Inch Plate

SECTION VII

SUMMARY AND CONCLUSIONS

An approximate finite element formulation has been developed, to include effects of geometric and material nonlinearities in plate analysis, and applied to some simple plate examples. Results indicate that the method may form the basis of a reasonable approximate approach for investigating this type of behavior.

SECTION VIII

REFERENCES

1. Mallett, R. H., and Marcal, P. V., "Finite Element Analysis of Nonlinear Structures", Journal of the Structural Division, ASCE, Vol. 94, No. ST9, Sept. 1968, pp. 2081-2105.

2. Murray, D. W., and Wilson, E. L., "Large Deflection Plate Analysis by Finite Element", Journal of the Engineering Mechanics Division, A.S.C.E., Vol. 95, EM1, Feb., 1969, pp. 143-165.

3. Murray, D. W., and Wilson, E. L., "Finite Element Post-Buckling Analysis of Thin Elastic Plates", to be published in the Journal of AIAA.

4. Wilson, E. L., Finite Element Analysis of Two-Dimensional Structures, SESM report 63-2, University of California, Berkeley, 1963.

5. Felippa, C. A., Refined Finite Element Analysis of Linear and Non-linear Two-Dimensional Structures, SESM Report 66-22, University of California, Berkeley, 1966.

6. Khojasteh-Bakht, M., Analysis of Elastic-Plastic Shells of Revolution Under Axisymmetric Loading by the Finite Element Method, SESM Report 67-8, University of California, Berkeley, 1967.

7. Marcal, P. V. and Pilgrim, W. R., "Stiffness Method for Elastic-Plastic Shells of Revolution", J. Strain Analysis, 1, p. 339, 1966.